

See discussions, stats, and author profiles for this publication at: <https://www.researchgate.net/publication/5819317>

# Characterization of a New Class of Potent Inhibitors of the Voltage-Gated Sodium Channel Nav1.7

ARTICLE *in* BIOCHEMISTRY · JANUARY 2008

Impact Factor: 3.02 · DOI: 10.1021/bi7018207 · Source: PubMed

---

CITATIONS

47

---

READS

104

12 AUTHORS, INCLUDING:



**Scott B Hoyt**

Merck

30 PUBLICATIONS 318 CITATIONS

SEE PROFILE



**Clare London**

Merck

30 PUBLICATIONS 316 CITATIONS

SEE PROFILE



**Joseph L Duffy**

Merck

49 PUBLICATIONS 1,098 CITATIONS

SEE PROFILE

# Characterization of a New Class of Potent Inhibitors of the Voltage-Gated Sodium Channel Nav1.7

Brande S. Williams,<sup>‡,§</sup> John P. Felix,<sup>‡,§</sup> Birgit T. Priest,<sup>‡,§</sup> Richard M. Brochu,<sup>‡</sup> Kefei Dai,<sup>‡</sup> Scott B. Hoyt,<sup>||</sup> Clare London,<sup>||</sup> Yui S. Tang,<sup>⊥</sup> Joseph L. Duffy,<sup>||</sup> William H. Parsons,<sup>||</sup> Gregory J. Kaczorowski,<sup>‡</sup> and Maria L. Garcia<sup>\*,‡</sup>

*Departments of Ion Channels, Medicinal Chemistry, and Drug Metabolism, Merck Research Laboratories, P.O. Box 2000, Rahway, New Jersey 07065*

*Received September 5, 2007; Revised Manuscript Received October 10, 2007*

**ABSTRACT:** Voltage-gated sodium channels (Nav1) transmit pain signals from peripheral nociceptive neurons, and blockers of these channels have been shown to ameliorate a number of pain conditions. Because these drugs can have adverse effects that limit their efficacy, more potent and selective Nav1 inhibitors are being pursued. Recent human genetic data have provided strong evidence for the involvement of the peripheral nerve sodium channel subtype, Nav1.7, in the signaling of nociceptive information, highlighting the importance of identifying selective Nav1.7 blockers for the treatment of chronic pain. Using a high-throughput functional assay, novel Nav1.7 blockers, namely, the 1-benzazepin-2-one series, have recently been identified. Further characterization of these agents indicates that, in addition to high-affinity inhibition of Nav1.7 channels, selectivity against the Nav1.5 and Nav1.8 subtypes can also be achieved within this structural class. The most potent, nonselective member of this class of Nav1.7 blockers has been radiolabeled with tritium. [<sup>3</sup>H]BNZA binds with high affinity to rat brain synaptosomal membranes ( $K_d = 1.5$  nM) and to membranes prepared from HEK293 cells stably transfected with hNav1.5 ( $K_d = 0.97$  nM). In addition, and for the first time, high-affinity binding of a radioligand to hNav1.7 channels ( $K_d = 1.6$  nM) was achieved with [<sup>3</sup>H]BNZA, providing an additional means for identifying selective Nav1.7 channel inhibitors. Taken together, these data suggest that members of the novel 1-benzazepin-2-one structural class of Nav1 blockers can display selectivity toward the peripheral nerve Nav1.7 channel subtype, and with appropriate pharmacokinetic and drug metabolism properties, these compounds could be developed as analgesic agents.

Voltage-gated sodium channels (Nav1)<sup>1</sup> are responsible for the initiation and propagation of action potentials in excitable cells. Sodium channels mediate the initial inward current that causes rapid depolarization during the rising phase of the action potential, which in turn activates voltage-gated calcium and potassium channels. Sodium channels consist of a pore-forming  $\alpha$  subunit (~260 kDa), differentially expressed in different tissues, that can associate with one or two smaller auxiliary  $\beta$  subunits (1, 2). Genes encoding ten  $\alpha$  subunits and four  $\beta$  subunits have been identified. Although the  $\alpha$  subunit alone forms functional

channels with all of the major properties of native channels, i.e., selectivity and voltage-dependent activation and inactivation, coexpression with  $\beta$  subunits can result in higher expression levels, faster inactivation kinetics, or changes in steady-state voltage dependence (3–6). Nine of the identified  $\alpha$  subunits have been functionally expressed to date (7, 8).

Several pharmacological agents, including neurotoxins, antiarrhythmics, anticonvulsants, and local anesthetics, interact with the sodium channel  $\alpha$  subunit (9) by binding to residues contributed by the S5 and S6 pore-lining segments of the channel (10). Because this region of the channel is highly conserved among different channel subtypes (10, 11), most sodium channel blockers identified to date interact similarly with all channel subtypes tested. Despite their lack of molecular selectivity, sodium channel blockers, such as those used in the treatment of epilepsy (e.g., lamotrigine, phenytoin, and carbamazepine) and certain cardiac arrhythmias (e.g., lidocaine, tocainide, and mexiletine), display functional selectivity and an acceptable therapeutic index as a consequence of their preferential binding to open and inactivated states (12, 13) and their use-dependent block seen during high-frequency electrical activity. Voltage- and use-dependent properties appear to be critical for the ability of the drugs to block pathological firing patterns without significantly affecting normal firing activity.

\* To whom correspondence should be addressed. Phone: (732) 594-7564; Fax: (732) 594-3925; E-mail: maria\_garcia@merck.com.

<sup>‡</sup> Department of Ion Channels.

<sup>§</sup> These authors contributed equally to this work.

<sup>||</sup> Department of Medicinal Chemistry.

<sup>⊥</sup> Department of Drug Metabolism.

<sup>1</sup> Abbreviations: Nav1, voltage-dependent sodium channel; [<sup>3</sup>H]-BNZA, tritiated 1-benzazepin-2-one, compound 1; FRET, fluorescence resonance energy transfer; BPBTS, *N*-{[2'-(aminosulfonyl)biphenyl-4-yl]methyl}-*N'*-(2,2'-bithien-5-ylmethyl)succinamide; HEK, human embryonic kidney; (CC2-DMPE), *N*-(6-chloro-7-hydroxycoumarin-3-carbonyl)dimyristoylphosphatidylethanolamine; (DiSBAC<sub>2</sub>(3)), bis(1,3-diethylthiobarbituric acid)trimethine oxonol; WIN 17317-3, 1-benzyl-7-chloro-4-(*n*-pentylimino)-1,4-dihydroquinoline hydrochloride; HEPES, *N*-(2-hydroxyethyl)piperazine-*N'*-(2-ethanesulfonic acid); VIPR, voltage/ion probe reader; FLIPR, fluorimetric imaging plate reader.

More recently, sodium channels expressed in primary afferent neurons have been implicated in the aberrant firing patterns that follow nerve injury, suggesting that blockers of these channels could have utility in the treatment of neuropathic pain conditions (14, 15). Indeed, carbamazepine and Lidoderm, a topical formulation of the local anesthetic lidocaine, have been approved by the FDA for the treatment of trigeminal neuralgia and postherpetic neuralgia, respectively (16, 17). These agents block all sodium channel subtypes with similar potency and thus do not offer any insight into the subtype(s) responsible for pain signaling. Nav1.7, the product of the *SCN9A* gene, is present in nociceptive dorsal root ganglion neurons, and experimental evidence suggests a role for this channel in acute and inflammatory pain signaling. For instance, increased expression of Nav1.7 in dorsal root ganglion neurons following the administration of inflammatory mediators has been reported (18), and specific targeted deletion of Nav1.7 in dorsal root ganglion neurons reduces inflammatory responses in mice (19). In humans, mutations in Nav1.7 that increase channel activity are associated with familial erythromelalgia (20, 21), an inherited syndrome characterized by bouts of severe burning pain of the extremities in response to mild warmth, and with paroxysmal extreme pain disorder (22), an inherited condition characterized by attacks of rectal, ocular, or submandibular pain with flushing. Conversely, mutations that cause loss of Nav1.7 function have been linked to a congenital inability to experience pain with no apparent deficits in non-nociceptive sensory functions (23, 24). Given these data, potent and selective inhibitors of peripheral nerve sodium channels, in particular Nav1.7 channels, are expected to have an improved therapeutic index compared to currently used drugs for the treatment of pain associated with lesions or dysfunction of normal sensory pathways.

The search for novel sodium channel blockers has been hampered for a long time by the lack of appropriate high-throughput functional assays. Although electrophysiology has been the standard functional assay for sodium channels, its extremely low throughput has limited its use to the detailed characterization of a few chosen compounds. Recently, advances in fluorescence-based membrane-potential assays (25) and automated voltage clamp technologies (26) have enabled high- and medium-throughput functional evaluation of sodium channel blockers, respectively. Specifically, fluorescence resonance energy transfer (FRET) technology using membrane potential-sensitive dyes has been shown to provide a reliable assay of voltage-gated sodium channel activity in stably transfected cells expressing hNav1.5, hNav1.7, or hNav1.8 channels (27, 28). Using this assay, *N*-{[2'-(aminosulfonyl)biphenyl-4-yl]methyl}-*N'*-(2,2'-bithien-5-ylmethyl)succinamide (BPBTS), a member of a new class of disubstituted succinamide sodium channel blockers with efficacy in a rat pain model, was identified and characterized (29). BPBTS is a voltage- and use-dependent blocker and is 2 orders of magnitude more potent than anticonvulsant and antiarrhythmic sodium channel blockers currently used to treat neuropathic pain. Because the pharmacokinetic properties of this compound are not ideal, related analogues with similar potency and improved oral bioavailability were synthesized. Although these compounds do not exhibit molecular selectivity for any Nav1 subtype, they demonstrate efficacy in animal pain models without cardiac liabilities (30).

Recently, a novel structural family, the 1-benzazepin-2-ones, has been identified as Nav1.7 blockers (31, 32). In the spinal nerve ligation model of neuropathic pain, one of these agents reversed mechanical allodynia when dosed orally in rats. In the present study, we further characterize 1-benzazepin-ones and show that members of this class can display molecular selectivity between Nav1 channel subtypes. The nonselective blocker [<sup>3</sup>H]BNZA binds with high affinity to neuronal sodium channels and to hNav1.5 channels stably expressed in HEK293 cells. In addition, hNav1.7 channels were characterized for the first time with the use of [<sup>3</sup>H]-BNZA, suggesting the utility of this ligand in the development of Nav1.7 channel pharmacology. Members of the 1-benzazepin-2-one class of Nav1.7 blockers with appropriate pharmacokinetic and drug metabolism properties could be developed as therapeutic agents.

## MATERIALS AND METHODS

**Materials.** Stable HEK293 cell lines expressing hNav1.5 or hNav1.7 channels were obtained from Dr. Hartman and Aurora Biosciences, respectively (27). The hNav1.7 HEK293 cell line was transfected with the  $\beta$ 1 subunit to yield a stable hNav1.7/ $\beta$ 1 cell line. An HEK293 cell line stably expressing hNav1.8 was prepared as described (28). All tissue culture media were obtained from Invitrogen Corp., Carlsbad, CA. For electrophysiological recordings, cells were plated on 35 mm dishes coated with poly-D-lysine. *N*-(6-Chloro-7-hydroxycoumarin-3-carbonyl)dimyristoylphosphatidylethanolamine (CC2-DMPE) and bis(1,3-diethylthiobarbituric acid)trimethine oxonol (DiSBAC<sub>2</sub>(3)) were purchased from Invitrogen Corp.; pluronic acid was obtained from Molecular Probes, Eugene, OR. Deltamethrin was purchased from Crescent Chemical Corp., Islandia, NY, and brevetoxin from CalBiochem, San Diego, CA. Tetracaine hydrochloride, quinidine, flunarizine, phenytoin, and tetrodotoxin were obtained from Sigma-Aldrich, Saint Louis, MO. Veratridine and (*R*)-SDZ-201 were purchased from Biomol Research Laboratory Inc., Plymouth Meeting, PA. Synthesis of 1-benzazepin-2-one analogues was carried out as described (31, 32). BPBTS and WIN 17317-3 were prepared as previously described (29). All other reagents were obtained from commercial sources and were of the highest purity commercially available.

**Functional Nav1 Assays.** The functional activity of Nav1.5, Nav1.7, or Nav1.8 channels was measured as previously described (27, 28). Briefly, hNav1.5, hNav1.7, or hNav1.8 expressing cells were plated in poly-D-lysine-coated 96- or 384-well plates and incubated overnight at 37 °C in a 10% CO<sub>2</sub> atmosphere in growth medium. The cells were washed with Dulbecco's phosphate-buffered saline (D-PBS) containing calcium and magnesium and incubated with CC2-DMPE and pluronic acid in D-PBS with calcium and magnesium, supplemented with 10 mM glucose and 10 mM HEPES—NaOH, pH 7.4. After incubation in the dark at 25 °C, the cells were washed and incubated in 165 mM NaCl, 4.5 mM KCl, 2 mM CaCl<sub>2</sub>, 1 mM MgCl<sub>2</sub>, 10 mM glucose, 10 mM HEPES—NaOH, pH 7.4, containing DiSBAC<sub>2</sub>(3), in the dark at 25 °C, in the absence or presence of the test compound. At the end of the incubation period, the plates were placed in either a VIPR instrument (Aurora Biosciences Corp., San Diego, CA) or an FLIPR-Tetra instrument (Molecular Devices, Sunnyvale, CA). The cells were illuminated at 400

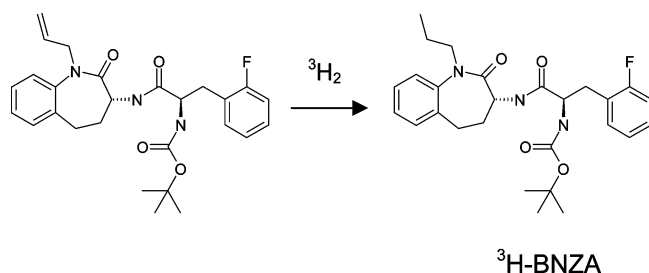
nm, and fluorescence emissions were recorded at 460 and 580 nm. After baseline emissions were recorded, a solution containing appropriate concentrations of sodium channel agonist was added, and the emissions of both dyes were recorded for an additional period of time. The change in FRET ratio ( $F/F_0$ ) was calculated as

$$F/F_0 = [(A_{460}/A_{580})/(I_{460}/I_{580})]$$

where  $A$  and  $I$  represent the fluorescence emission at the specified wavelength after or before addition of agonist, respectively.

**Electrophysiology.** Sodium currents were examined by whole cell voltage clamp (33) using an EPC-9 amplifier and Pulse software (HE Electronics, Lamprecht, Germany). All experiments were performed at room temperature. Electrodes were fire-polished to resistances of 1.5–4 M $\Omega$ . Voltage errors were minimized by series resistance compensation (75–85%), and the capacitance artifact was canceled using the amplifier's built-in circuitry. Data were acquired at 50 kHz and filtered at 10 kHz. The extracellular solution consisted of 160 mM NaCl, 1 mM KCl, 2.7 mM CaCl<sub>2</sub>, 0.5 mM MgCl<sub>2</sub>, 10 mM NMDG-HEPES, pH 7.4, and the internal (pipet) solution contained 110 mM cesium methanesulfonate, 5 mM NaCl, 20 mM CsCl, 10 mM CsF, 10 mM BAPTA (tetracesium salt), 10 mM Cs-HEPES, pH 7.4. In some cases, NaCl in the bath solution was partially replaced by (NMDG)Cl to avoid artifacts caused by large current amplitudes.

**Synthesis of [<sup>3</sup>H]BNZA.** The precursor for radiolabeling was synthesized as described previously (31). A solution of 5 mg of precursor in 0.8 mL of anhydrous DMF was degassed at dry ice/acetone temperature in the presence of 5 mg of 10% Pd/C (Aldrich Chemical). The mixture was stirred at ice temperature for 2 h under 240 mmHg of carrier-free tritium gas (1.2 Ci, American Radiochemical Chemicals). Any unreacted tritium gas was removed, the catalyst was filtered through a syringeless filter device (Whatman Autovial, 0.45  $\mu$ m PTFE), and the solvent and labile tritiums were concentrated to near dryness. The dried residue was resuspended in 2 mL of ethanol and subjected to HPLC (Zorbax, SBCN HPLC column, 9.4 mm  $\times$  25 cm, CH<sub>3</sub>CN:H<sub>2</sub>O:TFA = 25:75:0.1 to 27:73:0.1 in 50 min). [<sup>3</sup>H]BNZA, which eluted with a retention time of 48 min (the unreacted precursor eluted at 47 min), was assayed by analytical HPLC, Zorbax SBCN column at CH<sub>3</sub>CN:H<sub>2</sub>O:TFA = 25:75:0.1, to be 99% radiochemically pure and to have a specific activity of 30 Ci/mmol. The total radiochemical yield was 302 mCi.



**Binding Assay.** Rat brain synaptosomal plasma membrane vesicles and membranes from HEK293 cells stably transfected with hNav1.5, hNav1.7/ $\beta$ 1, or hNav1.8 were prepared as previously described (34) and stored at –70 °C. Binding

of [<sup>3</sup>H]BNZA was monitored at room temperature in borosilicate glass tubes containing 100 mM NaCl, 20 mM Tris-HCl, pH 7.4, supplemented with 0.01% bovine serum albumin. For saturation experiments, the membranes were incubated with increasing concentrations of [<sup>3</sup>H]BNZA at room temperature for at least 5 h. To determine the kinetics of ligand association, the membranes were incubated with [<sup>3</sup>H]BNZA for different periods of time at room temperature. Ligand dissociation was initiated by addition of 1–10  $\mu$ M unlabeled BNZA. Nonspecific binding was determined in the presence of 1  $\mu$ M unlabeled BNZA. Separation of bound from free ligand was achieved by diluting the samples with 4 mL of ice-cold buffer consisting of 100 mM NaCl, 20 mM Tris-HCl, pH 7.4, 0.1% bovine serum albumin and filtering through GF/C glass fiber filters presoaked in quench buffer. The radioactivity retained on the filters was determined by liquid scintillation techniques. Data from saturation experiments were analyzed according to the equation  $B_{eq} = (B_{max}L^*)/(K_d + L^*)$ , where  $B_{eq}$  is the amount of ligand bound at equilibrium,  $B_{max}$  the maximum receptor concentration,  $K_d$  the ligand dissociation constant, and  $L^*$  the free ligand concentration. The association rate constant ( $k_1$ ) was determined from the equation  $k_1 = k_{obs}(B_{eq}/(L^*B_{max}))$ , where  $k_{obs}$  is the slope of the pseudo-first-order plot  $\ln(B_{eq}/(B_{eq} - B_t))$  versus time. The dissociation rate constant  $k_{-1}$  was calculated by fitting the data to a single monoexponential decay. IC<sub>50</sub> values for inhibition of [<sup>3</sup>H]BNZA binding were determined using the equation  $B_{eq} = (B_{max} - B_{min})/[1 + (I/IC_{50})^{n_H}] + B_{min}$ , where  $B_{max}$  is the binding with no inhibitors present,  $B_{min}$  is the amount of ligand bound at the maximal inhibitor concentration,  $I$  is the inhibitor concentration,  $n_H$  is the Hill coefficient, and IC<sub>50</sub> is the inhibitor concentration resulting in 50% inhibition. In most experiments,  $B_{max}$  was approximately 100% and  $B_{min}$  was typically close to 0%. Triplicate samples were determined for each experimental point. The standard deviation of the mean was typically less than 10%. Values are presented as the average  $\pm$  SE of several independent determinations.

## RESULTS

**Voltage-Gated Sodium Channel Blockers, 1-Benzazepin-2-ones, Display Subtype Selectivity.** High-throughput functional assays that monitor the activity of Nav1 channel subtypes have recently been developed (27, 28). These assays use voltage-dependent FRET between a pair of membrane-bound fluorescent probes to monitor changes in the membrane potential. Cells are preincubated with test compounds in physiological medium and then exposed to a sodium channel agonist that slows channel inactivation. Sodium ions moving through open channels lead to membrane depolarization that can be measured with the FRET dyes. Using this assay, a family of novel Nav1.7 channel blockers, 1-benzazepin-2-ones, has been identified (31, 32). Members of this family potently inhibit veratridine-mediated depolarization in HEK293 cells stably expressing hNav1.7 channels (Figure 1, Table 1). Figure 1A shows the fluorescence emissions from CC2-DMPE and DiSBAC<sub>2</sub>(3), the fluorescence emission ratio upon addition of 25  $\mu$ M veratridine, and a representative example of FRET inhibition by increasing concentrations of compound 4. Figure 1B illustrates concentration-dependent inhibition of the FRET signal as a function of the compound concentration. The solid lines



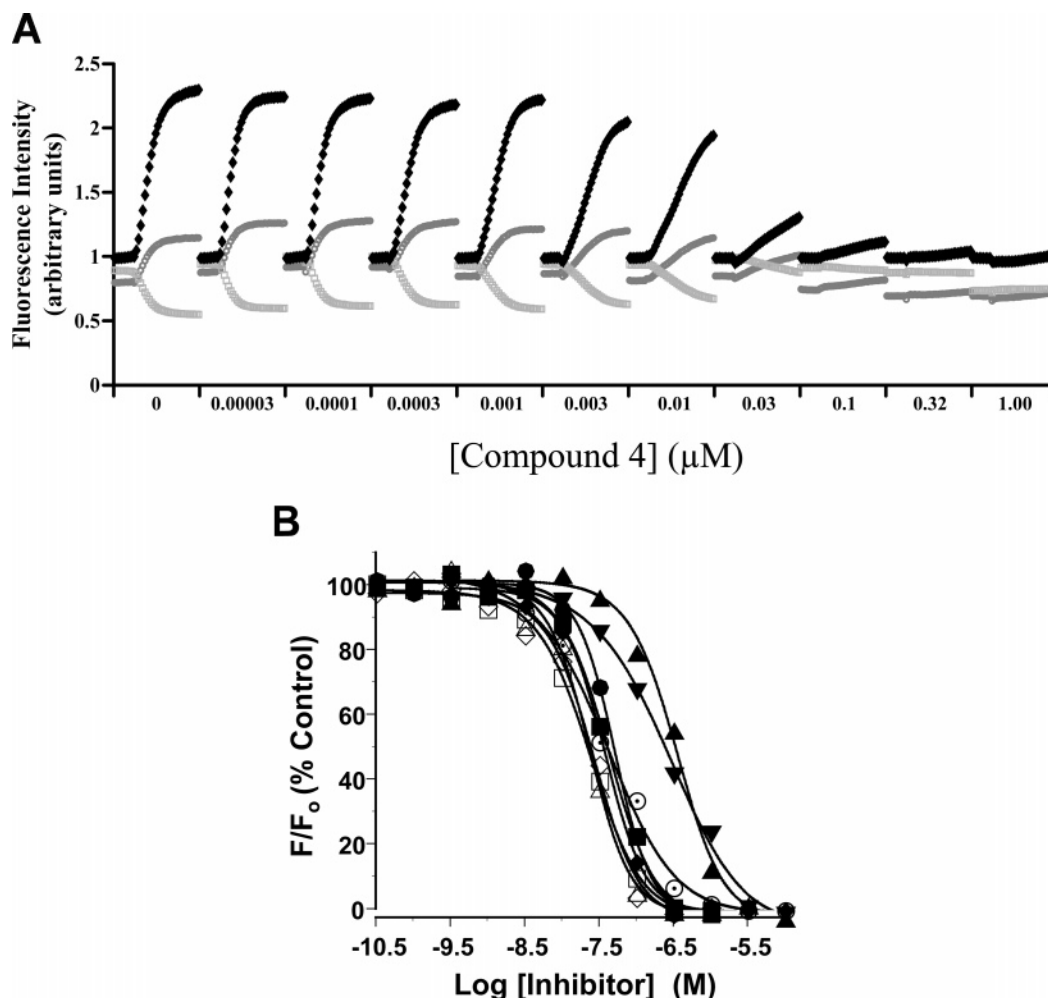


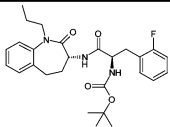
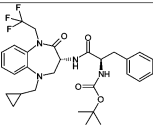
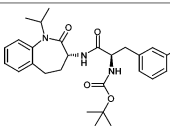
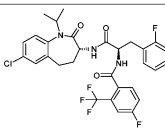
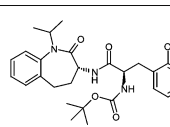
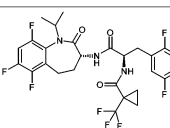
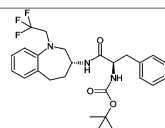
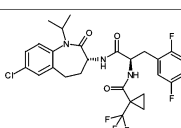
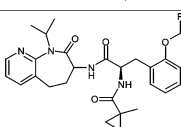
FIGURE 1: Inhibition of hNav1.7 channels by 1-benzazepin-2-one analogues. HEK293 cells stably transfected with hNav1.7 were plated in 96-well plates and incubated with the FRET dyes in physiological medium, as described in the Materials and Methods, in the absence or presence of increasing concentrations of compound. (A) Upon recording the emission of both dyes (gray lines) for 7 s at 1 Hz, veratridine was added at a final concentration of 25  $\mu\text{M}$ , and fluorescence from both dyes was monitored for an additional 33 s at 1 Hz. The bold line represents FRET defined as the ratio of CC2-DMPE to DiSBAC<sub>2</sub>(3). Increasing concentrations of compound 4 cause inhibition of the FRET signal. (B) Inhibition of hNav1.7 by compounds 1–9. Data are presented as the percentage of inhibition of the FRET signal relative to an untreated control. Fitting to the Hill equation yielded  $\text{IC}_{50}$  values of 0.027  $\mu\text{M}$  ( $\diamond$ ), 0.024  $\mu\text{M}$  ( $\triangle$ ), 0.042  $\mu\text{M}$  ( $\blacksquare$ ), 0.024  $\mu\text{M}$  ( $\square$ ), 0.051  $\mu\text{M}$  ( $\bullet$ ), 0.038  $\mu\text{M}$  ( $\blacklozenge$ ), 0.037  $\mu\text{M}$  ( $\odot$ ), 0.273  $\mu\text{M}$  ( $\blacktriangledown$ ), and 0.345  $\mu\text{M}$  ( $\blacktriangle$ ).

represent the best fit of the data to the Hill equation, and average  $\text{IC}_{50}$  values for inhibition from several independent experiments are presented in Table 1. Interestingly, when the same compounds are tested against other Nav1 channel subtypes, different patterns of activity emerge (Table 1). Thus, while all compounds display lower affinity for hNav1.8, only selected compounds appear less potent on hNav1.5. The finding that 1-benzazepin-2-one analogues are less potent on Nav1.8 than Nav1.7 channels is not related to the nature of the functional assay since other well-characterized Nav1 inhibitors do not display differences between these two Nav1 channel subtypes (27, 28). These data indicate that 1-benzazepin-2-one analogues are potent Nav1.7 inhibitors and possess selectivity against the peripheral nerve Nav1.8 channel, with some family members also being able to discriminate against the cardiac Nav1.5 channel. One of the 1-benzazepin-2-one analogues, compound 4, was selected for further characterization. Compound 4 was tested in radioligand binding assays against other ion channels as well as numerous receptors and enzymes. Compound 4 had weak activity against L-type calcium channels, on the basis of its

effect on [ $^3\text{H}$ ]diltiazem binding to rabbit skeletal muscle membranes ( $\text{IC}_{50} \approx 1 \mu\text{M}$ ). At a concentration of 10  $\mu\text{M}$ , compound 4 inhibited [ $^3\text{H}$ ]MK-0499 binding to membranes derived from HEK293 cells stably expressing hERG by 31%. Evaluation of compound 4 (10  $\mu\text{M}$ ) in over 100 receptor ligand binding and enzymatic assays in a standard PanLabs screen (MDS Pharma Services, Taiwan) yielded few significant interactions. Of these, the most notable involved inhibition of acetyl cholinesterase ( $\text{IC}_{50} = 1.7 \mu\text{M}$ ), protein tyrosine and protein serine/threonine kinases ( $\text{IC}_{50} = 1.7$  and 2.8  $\mu\text{M}$ , respectively), oxytocin receptor ( $\text{IC}_{50} = 3.7 \mu\text{M}$ ), adenosine A3 ( $\text{IC}_{50} = 5.3 \mu\text{M}$ ), tachykinin NK2 ( $\text{IC}_{50} = 6.5 \mu\text{M}$ ), and the cannabinoid receptor CB2 ( $\text{IC}_{50} = 7.0 \mu\text{M}$ ). On this basis, compound 4 appears to display good selectivity for Nav1.7 channels.

**Block of Recombinant Nav1 Channels by 1-Benzazepin-2-ones.** The interactions of compounds 1 and 4 with Nav1.7, Nav1.8, or Nav1.5 channels were further characterized in whole cell electrophysiology. Bath application of compound 1 reversibly blocked hNav1.7 channels, and block was dependent on the holding potential as shown in the traces in

Table 1. Inhibition of hNav1.7, hNav1.5, or hNav1.8 Channels by 1-Benzazepin-2-one Compounds **1**–**9**<sup>a</sup>

	Structure	hNav1.7	hNav1.5	hNav1.8
Compound 1		0.03 ± 0.01	0.02 ± 0.01	0.27 ± 0.06
Compound 2		0.03 ± 0.01	0.02 ± 0.00	0.13 ± 0.01
Compound 3		0.03 ± 0.02	0.05 ± 0.02	0.72 ± 0.46
Compound 4		0.03 ± 0.02	0.18 ± 0.05	0.30 ± 0.16
Compound 5		0.03 ± 0.01	0.03 ± 0.01	0.50 ± 0.09
Compound 6		0.05 ± 0.02	0.20 ± 0.07	0.53 ± 0.19
Compound 7		0.09 ± 0.05	0.87 ± 0.35	0.68 ± 0.12
Compound 8		0.39 ± 0.22	1.75 ± 0.08	1.36 ± 0.38
Compound 9		0.48 ± 0.18	5.51 ± 2.57	>10

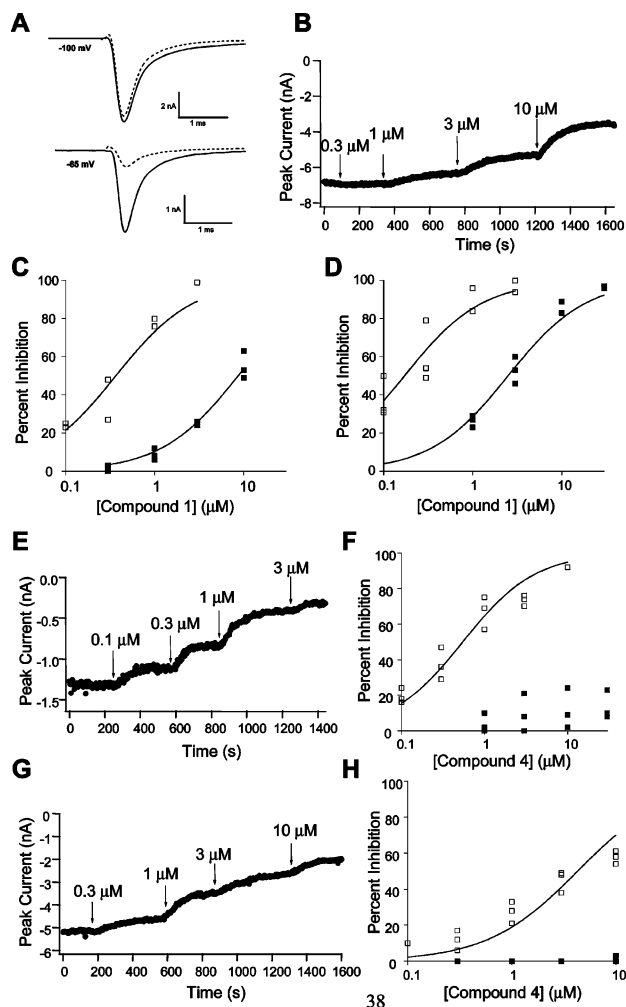
<sup>a</sup> IC<sub>50</sub> values for inhibition were determined as indicated in the Materials and Methods and represent the means ± SD of at least three independent experiments.

Figure 2A,C. The current evoked by short depolarizations from −100 mV was blocked with an IC<sub>50</sub> of 8.7 μM, whereas the current evoked from a holding potential of −65 mV was blocked with an IC<sub>50</sub> of 0.37 μM. At physiological pH, compound **1** is not charged, and the dependence of block on the holding potential is presumably due to a preferential interaction with channels in the inactivated state (29, 35, 36). At −100 mV, hNav1.7 channels reside primarily in the resting state, whereas approximately half of the channels are inactivated at −65 mV. Compound **1** interacted in a similar manner with hNav1.5 channels (Figure 2D), blocking channels with IC<sub>50</sub> values of 2.5 and 0.17 μM, at holding potentials of −110 and −75 mV, respectively. As expected from the fluorescent assay, block of hNav1.8 channels was somewhat weaker with IC<sub>50</sub> values of 7.5 and 0.99 μM, at holding potentials of −100 and −55 mV, respectively (data

not shown). Holding potentials were chosen to match the fraction of inactivated channels for the different Nav1 subtypes tested.

When compound **4** was bath applied to hNav1.7 channels at −100 mV, minimal block was seen even at the highest concentration tested (10 μM), whereas the IC<sub>50</sub> for block at −65 mV (0.55 μM) was similar to that for compound **1** (Figure 2E,F), suggesting that compound **4** interacts more selectively with channels in the inactivated state. In agreement with observations in the fluorescent assay, compound **4** blocked hNav1.5 and hNav1.8 channels more weakly than hNav1.7 channels, resulting in an IC<sub>50</sub> for block at −75 mV of 4.3 μM for hNav1.5 (Figure 2G,H) and an IC<sub>50</sub> for block at −55 mV of 5.5 μM for hNav1.8 (data not shown).

**Binding of [<sup>3</sup>H]BNZA to Rat Brain Membranes.** To further characterize the interaction of 1-benzazepin-2-one com-



**FIGURE 2:** Block of Nav1 channels by 1-benzazepin-2-ones. Block of hNav1.7 and hNav1.5 channels by compounds **1** and **4** was examined by whole cell voltage clamp. (A) Representative hNav1.7 currents in response to voltage steps to +10 mV from  $-100$  or  $-65$  mV are shown in the control and in the presence of  $1 \mu\text{M}$  compound **1**. (B) Peak hNav1.7 currents elicited by steps to +10 mV from  $-100$  mV were measured in the presence of increasing concentrations of compound **1** as indicated. (C) Inhibition of hNav1.7 currents as a function of the compound **1** concentration for holding potentials of  $-100$  mV (filled squares) and  $-65$  mV (open squares). Fitting the Hill equation ( $n_H = 1$ ) to the data yielded  $\text{IC}_{50}$  values of  $8.7$  and  $0.37 \mu\text{M}$  for holding potentials of  $-100$  and  $-65$  mV, respectively. (D) Inhibition of hNav1.5 currents as a function of the compound **1** concentration for holding potentials of  $-110$  mV (filled squares) and  $-75$  mV (open squares). Fitting the Hill equation ( $n_H = 1$ ) to the data yielded  $\text{IC}_{50}$  values of  $2.5$  and  $0.17 \mu\text{M}$  for holding potentials of  $-110$  and  $-75$  mV, respectively. (E) Peak hNav1.7 currents elicited by steps to +10 mV from  $-65$  mV were measured in the presence of increasing concentrations of compound **4**. (F) Inhibition of hNav1.7 currents as a function of the compound **4** concentration for holding potentials of  $-100$  mV (filled squares) and  $-65$  mV (open squares). Fitting the Hill equation ( $n_H = 1$ ) to the data yielded an  $\text{IC}_{50}$  of  $0.55 \mu\text{M}$ . (G) Peak hNav1.5 currents elicited by steps to +10 mV from  $-75$  mV were measured in the presence of increasing concentrations of compound **4**. (H) Inhibition of hNav1.5 currents as a function of the compound **4** concentration for holding potentials of  $-110$  mV (filled squares) and  $-75$  mV (open squares). Fitting the Hill equation ( $n_H = 1$ ) to the data yielded an  $\text{IC}_{50}$  of  $4.3 \mu\text{M}$ . In (C), (D), (F), and (H), data from three cells at each voltage and concentration are shown, and the Hill equation is the fit to all data points.

pounds with voltage-gated sodium channels, compound **1** (BNZA) was radiolabeled with tritium, and its interaction

with rat neuronal sodium channels was determined. Under equilibrium conditions, specific binding of [ $^3\text{H}$ ]BNZA to rat brain synaptosomal membranes reaches saturation and displays a good signal-to-noise ratio (Figure 3A). Fitting the specific binding data to a single-site model yielded a  $K_d$  of  $1.53 \pm 0.46 \text{ nM}$  and a  $B_{\text{max}}$  of  $3.4 \pm 1.2 \text{ pmol/mg}$  of protein ( $n = 6$ ).  $B_{\text{max}}$  values are similar to those of other sodium channel ligands, such as [ $^3\text{H}$ ]WIN 17317-3 and [ $^3\text{H}$ ]BPBTS (37). Unlabeled BNZA displaced [ $^3\text{H}$ ]BNZA binding to brain membranes with a  $K_i$  value of  $2.85 \pm 0.83 \text{ nM}$  and a Hill slope of  $1.0 \pm 0.1$  ( $n = 15$ ) (Figure 3D).

Binding of [ $^3\text{H}$ ]BNZA to rat brain membranes is a time-dependent process that reaches equilibrium in approximately 4 h at room temperature (Figure 3B). Linear transformation of these data, according to a pseudo-first-order reaction (inset), yielded a  $k_{\text{obs}}$  of  $0.017 \text{ min}^{-1}$ , corresponding to an association rate constant,  $k_1$ , of  $1 \times 10^7 \text{ M}^{-1} \text{ min}^{-1}$ . When  $k_1$  is calculated from a plot of  $k_{\text{obs}}$  versus ligand concentration, a similar value of  $1.1 \times 10^7 \text{ M}^{-1} \text{ min}^{-1}$  is obtained (data not shown). Dissociation of receptor-bound ligand, initiated by addition of excess unlabeled ligand, followed monoexponential kinetics, in agreement with a first-order reaction, and displayed  $k_{-1}$  values of  $0.015 \pm 0.004 \text{ min}^{-1}$  ( $n = 2$ ) (Figure 3C). The equilibrium dissociation constant calculated from these rate constants,  $1.5 \text{ nM}$ , is close to that determined under equilibrium binding conditions, suggesting that [ $^3\text{H}$ ]BNZA interaction with rat brain membranes is a bimolecular, fully reversible reaction. Although dissociation rates of another sodium channel ligand, [ $^3\text{H}$ ]BPBTS, have been shown to be highly dependent on the concentration of unlabeled compound used to block the association reaction, suggesting the existence of multiple attachment points between the ligand and its receptor (29), this phenomenon does not appear to be a feature of [ $^3\text{H}$ ]BNZA interaction with rat brain membranes. Thus,  $k_{-1}$  values determined in the presence of  $0.1$ ,  $1$ , or  $10 \mu\text{M}$  unlabeled BNZA ( $0.010$ ,  $0.015$ , and  $0.019 \text{ min}^{-1}$ , respectively) only differ by  $\sim 2$ -fold.

The pharmacological properties of [ $^3\text{H}$ ]BNZA binding to rat brain membranes were determined using different classes of sodium channel modulators. All of these agents inhibit binding of [ $^3\text{H}$ ]BNZA to brain membranes in a concentration-dependent manner (Figure 3D and data not shown) and display  $K_i$  values that are similar to those found in competition experiments with other well-characterized sodium channel ligands, such as [ $^3\text{H}$ ]WIN 17317-3 (37), [ $^3\text{H}$ ]BPBTS (29), and [ $^3\text{H}$ ]batrachotoxin (38). The compounds evaluated include sodium channel agonists (veratridine,  $K_i = 6.8 \pm 2.4 \mu\text{M}$ ,  $n = 2$ ; deltamethrin,  $K_i = 188 \pm 76 \text{ nM}$ ,  $n = 2$ ), antiarrhythmic agents (quinidine,  $K_i = 4.4 \pm 1.6 \mu\text{M}$ ,  $n = 3$ ; mexiletine,  $K_i = 4.6 \pm 2.3 \mu\text{M}$ ,  $n = 2$ ), cardiotonic agents (R(+)-SDZ-201,  $K_i = 10.4 \pm 4.5 \text{ nM}$ ,  $n = 3$ ), calcium channel modifiers (flunarizine,  $K_i = 9.1 \pm 1.6 \text{ nM}$ ,  $n = 3$ ), local anesthetics (tetracaine,  $K_i = 740 \pm 455 \text{ nM}$ ,  $n = 3$ ), anticonvulsants (phenytoin,  $K_i = 8 \pm 1 \mu\text{M}$ ,  $n = 4$ ), and the sodium channel blockers (WIN 17317-3,  $K_i = 3.8 \pm 1.3 \text{ nM}$ ,  $n = 3$ ; BIII 890 CL,  $K_i = 2.0 \pm 0.9 \text{ nM}$ ,  $n = 3$ ). Taken together, these data suggest that [ $^3\text{H}$ ]BNZA binds in a bimolecular, fully reversible reaction to a single class of high-affinity sites in rat brain membranes that display pharmacological features consistent with neuronal voltage-gated sodium channels.

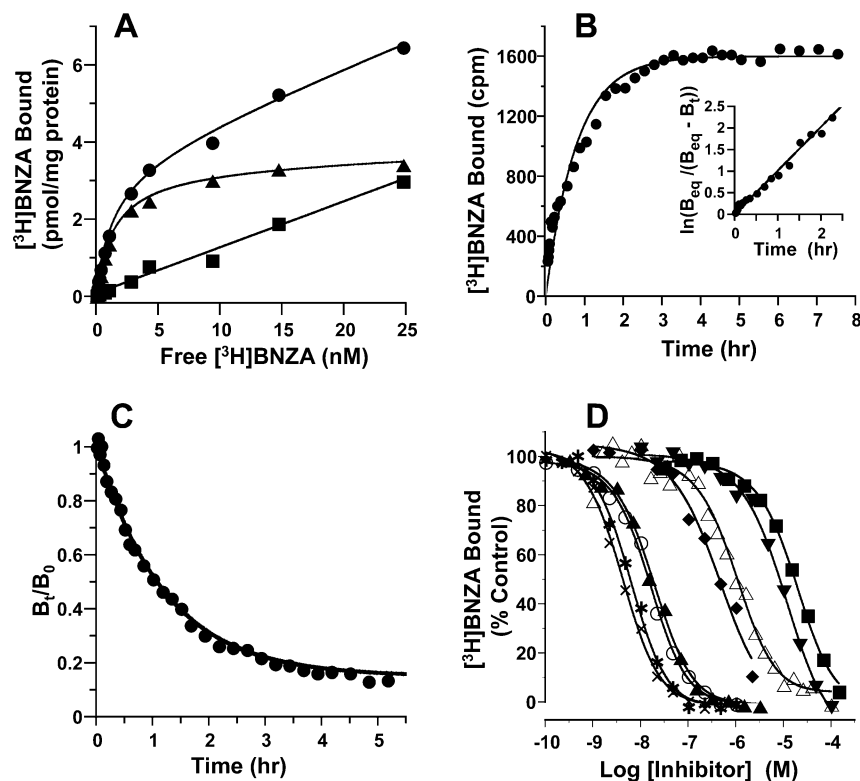


FIGURE 3: Binding of [ $^3\text{H}$ ]BNZA to rat brain synaptosomal membranes. (A) Rat brain membrane vesicles were incubated with increasing concentrations of [ $^3\text{H}$ ]BNZA for  $\sim 18$  h at room temperature. Specific binding data ( $\blacktriangle$ ) were assessed from the difference between total ( $\bullet$ ) and nonspecific ( $\blacksquare$ ) binding. For this experiment a  $K_d$  of 1.58 nM, a  $B_{\text{max}}$  of 3.5 pmol/mg of protein, and a Hill coefficient of 0.99 were determined. (B) Rat brain membranes were incubated with 1 nM [ $^3\text{H}$ ]BNZA for different periods of time at room temperature. Nonspecific binding was time invariant and has been subtracted from the experimental points. Inset: Linear transformation of specific binding data according to the pseudo-first-order reaction yielded  $k_{\text{obs}} = 0.017 \text{ min}^{-1}$ , corresponding to a  $k_1$  of  $1 \times 10^7 \text{ M}^{-1} \text{ min}^{-1}$ . (C) Rat brain synaptosomal membranes were incubated with 1 nM [ $^3\text{H}$ ]BNZA, and dissociation was initiated by addition of  $1 \mu\text{M}$  unlabeled BNZA. The samples were incubated at room temperature for the indicated periods of time. Data were fit to a single monoexponential decay, yielding a  $k_{-1}$  of  $0.014 \text{ min}^{-1}$ , corresponding to a  $t_{1/2}$  of dissociation of 48 min. (D) Rat brain membranes were incubated with  $\sim 1$  nM [ $^3\text{H}$ ]BNZA in the absence or presence of increasing concentrations of unlabeled BNZA ( $\times$ ), WIN 17317-3 ( $*$ ), flunarizine ( $\circ$ ), R(+)-SDZ-201 ( $\blacktriangle$ ), deltamethrin ( $\blacklozenge$ ), tetracaine ( $\triangle$ ), quinidine ( $\blacktriangledown$ ), or phenytoin ( $\blacksquare$ ) for 18 h at room temperature. Inhibition of binding was assessed relative to an untreated control. Data were fit to a single-site inhibition model, yielding  $\text{IC}_{50}$  values of ( $\times$ ) 5.0 nM, ( $*$ ) 6 nM, ( $\circ$ ) 15 nM, ( $\blacktriangle$ ) 19 nM, ( $\blacklozenge$ )  $0.38 \mu\text{M}$ , ( $\triangle$ )  $1.05 \mu\text{M}$ , ( $\blacktriangledown$ )  $10.2 \mu\text{M}$ , and ( $\blacksquare$ )  $21.3 \mu\text{M}$ .

**Binding of [ $^3\text{H}$ ]BNZA to hNav1.7 and hNav1.5 Channels.** Although [ $^3\text{H}$ ]BPBTS binds with high affinity to rat brain sodium channels and to cardiac Nav1.5 channels stably expressed in HEK293 cells, binding of this ligand could not be detected to membranes derived from the hNav1.7 HEK293 cell line. Indeed, high-affinity ligands with which to study Nav1.7 channels have not yet been disclosed. Having determined that [ $^3\text{H}$ ]BNZA is an appropriate ligand for studying native brain sodium channels, its utility for characterizing Nav1.7 channels was investigated. Incubation of [ $^3\text{H}$ ]BNZA with membranes derived from the hNav1.7/ $\beta 1$  HEK293 cell line leads to specific ligand association to a single class of sites that displays a  $K_d = 1.60 \pm 0.17$  nM and a  $B_{\text{max}}$  of  $1.3 \pm 0.9$  pmol/mg of protein ( $n = 3$ ) (Figure 4A). Binding of [ $^3\text{H}$ ]BNZA to hNav1.7/ $\beta 1$  membranes displays characteristics similar to those seen with rat brain membranes. Thus, [ $^3\text{H}$ ]BNZA binding is a time-dependent and fully reversible process characterized by  $k_1$  and  $k_{-1}$  values of  $5.3 \times 10^6 \text{ M}^{-1} \text{ min}^{-1}$  and  $0.0063 \text{ min}^{-1}$ , respectively (Figure 4B,C). Both values are approximately 2–3-fold different from those determined for rat brain membranes (see above), although the equilibrium binding constants,  $K_d$ , are similar. Other sodium channel modulators that inhibit binding of [ $^3\text{H}$ ]BNZA to brain membranes were also found to inhibit with similar potencies the interaction of [ $^3\text{H}$ ]BNZA

with hNav1.7/ $\beta 1$  membranes (veratridine,  $K_i = 11.9 \pm 2.8 \mu\text{M}$ ,  $n = 2$ ; deltamethrin,  $K_i = 185 \pm 33$  nM,  $n = 2$ ; quinidine,  $K_i = 8.5 \pm 2.7 \mu\text{M}$ ,  $n = 3$ ; mexiletine,  $K_i = 11.8 \pm 7.4 \mu\text{M}$ ,  $n = 2$ ; R(+)-SDZ-201,  $K_i = 21$  nM; flunarizine,  $K_i = 20.3 \pm 1.7$  nM,  $n = 3$ ; tetracaine,  $K_i = 1.7 \pm 0.6 \mu\text{M}$ ,  $n = 3$ ; phenytoin,  $K_i = 14.5 \pm 6.9 \mu\text{M}$ ,  $n = 2$ ; WIN 17317-3,  $K_i = 10.8 \pm 3.8$  nM,  $n = 3$ ; BIII 890 CL,  $K_i = 1.9 \pm 1.1$  nM,  $n = 4$ ) (Figure 4D). Several 1-benzazepin-2-one Nav1.7 inhibitors cause concentration-dependent inhibition of [ $^3\text{H}$ ]BNZA binding to hNav1.7/ $\beta 1$  membranes with a well-defined range of  $K_i$  values. One of the most potent compounds in the functional, membrane-potential-based hNav1.7 assay, compound **2**, displays the highest affinity ( $K_i = 0.37 \pm 0.04$  nM,  $n = 3$ ) in the binding assay (Figure 5).

High-affinity binding of [ $^3\text{H}$ ]BNZA also occurs to hNav1.5 channels. In this case, [ $^3\text{H}$ ]BNZA binds to a single class of sites present in membranes derived from HEK293 cells stably expressing the channel with  $K_d$ ,  $B_{\text{max}}$ , and  $n_H$  values of  $0.97 \pm 0.35$  nM,  $0.74 \pm 0.21$  pmol/mg of protein, and  $0.99 \pm 0.10$  ( $n = 3$ ), respectively. However, binding of [ $^3\text{H}$ ]BNZ to hNav1.8 channels could not be detected under many experimental conditions (data not shown) consistent with the lower affinity of 1-benzazepin-2-ones for this channel subtype. These data, taken together, illustrate for the first time the utility of a high-affinity ligand, [ $^3\text{H}$ ]BNZA, for



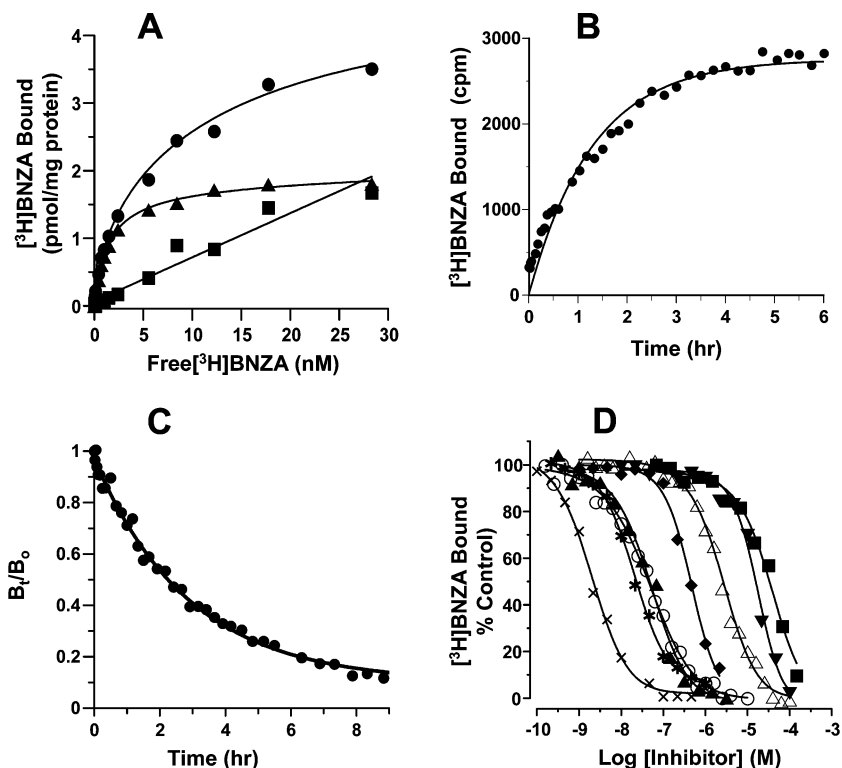


FIGURE 4: Binding of  $[^3\text{H}]\text{BNZA}$  to hNav1.7/ $\beta 1$  membranes. (A) Membranes prepared from HEK293 cells stably transfected with hNav1.7/ $\beta 1$  were incubated with increasing concentrations of  $[^3\text{H}]\text{BNZA}$  for 18 h at room temperature. Specific binding data (▲) were assessed from the difference between total (●) and nonspecific (■) binding. For this experiment, a  $K_d$  of 1.6 nM, a  $B_{\text{max}}$  of 1.98 pmol/mg of protein, and a Hill coefficient of 0.91 were determined. (B) hNav1.7/ $\beta 1$  membranes were incubated with 0.95 nM  $[^3\text{H}]\text{BNZA}$  for different periods of time at room temperature. Nonspecific binding was time invariant and has been subtracted from the experimental points. Inset: Linear transformation of specific binding data according to the pseudo-first-order reaction yielded  $k_{\text{obs}} = 0.01 \text{ min}^{-1}$ , corresponding to a  $k_1$  of  $4.8 \times 10^6 \text{ M}^{-1} \text{ min}^{-1}$ . (C) hNav1.7/ $\beta 1$  membranes were incubated with 0.95 nM  $[^3\text{H}]\text{BNZA}$ , and dissociation kinetics were initiated by addition of  $1 \mu\text{M}$  unlabeled BNZA. The samples were incubated at room temperature for the indicated periods of time. Data were fit to a single monoexponential decay, yielding a  $k_{-1}$  of  $0.0056 \text{ min}^{-1}$ , corresponding to a  $t_{1/2}$  of dissociation of 120 min. (D) Membranes were incubated with  $\sim 1 \text{ nM}$   $[^3\text{H}]\text{BNZA}$  in the absence or presence of increasing concentrations of unlabeled BNZA (×), WIN 17317-3 (\*), flunarizine (○), R(+)-SDZ-201 (▲), deltamethrin (◆), tetracaine (△), quinidine (▼), or phenytoin (■) for 18 h at room temperature. Inhibition of binding was assessed relative to an untreated control. Data were fit to a single-site inhibition model, yielding  $\text{IC}_{50}$  values of (×) 3 nM, (\*) 19 nM, (○) 45 nM, (▲) 49 nM, (◆)  $0.40 \mu\text{M}$ , (△)  $2.48 \mu\text{M}$ , (▼)  $16.6 \mu\text{M}$ , and (■)  $75.2 \mu\text{M}$ .

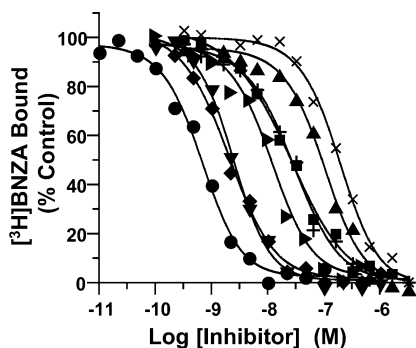


FIGURE 5: Inhibition of  $[^3\text{H}]\text{BNZA}$  binding to hNav1.7/ $\beta 1$  membranes by 1-benzazepin-2-one analogues. Membranes were incubated with  $\sim 1 \text{ nM}$   $[^3\text{H}]\text{BNZA}$  in the absence or presence of increasing concentrations of compound 2 (●), unlabeled BNZA (◆), compound 5 (▼), compound 6 (sideways triangle), compound 4 (■), compound 7 (+), compound 9 (▲), or compound 8 (×) for 18 h at room temperature. Inhibition of binding was assessed relative to an untreated control. Data were fit to a single-site inhibition model, yielding  $\text{IC}_{50}$  values of 0.7 nM (●), 2 nM (◆), 2.3 nM (▼), 10 nM (sideways triangle), 23.5 nM (■), 45 nM (+), 108 nM (▲), and 164 nM (×).

studying Nav1.7 channels and defining their pharmacology. In addition, the ability of  $[^3\text{H}]\text{BNZA}$  to bind to brain and cardiac Nav1.5 channels provides an additional tool with which to identify Nav1-subtype-selective inhibitors.

## DISCUSSION

The results reported herein concern the characterization of 1-benzazepin-2-ones, a novel and potent class of inhibitors of the peripheral nerve sodium channel, Nav1.7. In membrane potential, FRET-based functional assays, these compounds display selectivity against another peripheral nerve sodium channel, Nav1.8. In addition, some family members also display selectivity against the cardiac Nav1.5 channel.  $[^3\text{H}]\text{BNZA}$ , a member of this class of inhibitors, was used to pharmacologically characterize for the first time a receptor site associated with Nav1.7 channels. The efficacy of the new class of Nav1.7 inhibitors in a neuropathic pain model is consistent with the critical role that Nav1.7 channels play in pain signaling and provides a new chemical platform for developing analgesics with an improved side-effect profile compared to that of current pain medications.

State-dependent sodium channel blockers have demonstrated therapeutic utility as anticonvulsants, antiarrhythmics, and local anesthetics, and recently their use in the treatment of a number of neuropathic pain conditions has expanded research to identify more potent and selective sodium channel inhibitors. Sodium channel blockers currently used in the clinic are associated with a number of side effects, which can become dose-limiting and prevent patients from achieving adequate treatment (39). Dose-limiting side effects

typically result from sodium channel block in the central nervous system and include ataxia and sedation. Currently used agents are relatively weak sodium channel blockers and are highly brain penetrant, emphasizing the need for more potent, selective, and potentially less brain penetrant therapies. Although none of the clinically used sodium channel blockers are subtype-selective, few cardiac side effects have been reported in patients without prior heart conditions.

The contribution of individual Nav1 channel subtypes to transmission of pain signals remains a subject of debate. In particular, Nav1.7 channels are preferentially expressed in nociceptive dorsal root ganglion neurons and sympathetic ganglion neurons and are believed to produce threshold currents close to resting potentials, therefore amplifying small depolarizations. To date, nine mutations in Nav1.7 have been shown to segregate with primary erythromelalgia, an autosomal dominant painful neuropathy that features burning pain of the extremities in response to warm stimuli or moderate exercise (40–45). These mutations cause gain of Nav1.7 function and, in the case of the F1449V mutation, can lower the threshold for single action potentials and high-frequency firing of dorsal root ganglion neurons (44). It is interesting to note that patients suffering from erythromelalgia benefit in their pain relief from the use of lidocaine and mexiletine (46, 47). Another autosomal dominant disorder, paroxysmal extreme pain disorder, results from mutations in Nav1.7 that cause gain of channel function by interfering with channel inactivation (22, 48). The sodium channel blocking anticonvulsant carbamazepine is effective in many patients with this syndrome. In addition, mutations that cause a loss of Nav1.7 function have been linked to a congenital inability to experience pain, providing supporting evidence for Nav1.7 as a critical contributor to nociception in humans (23, 24). The preliminary *in vivo* efficacy seen in pain animal models with 1-benzazepin-2-one Nav1.7 blockers argues that Nav1.7 channels are critical components of signaling in a wide variety of pain conditions (31, 32). It will be interesting to see how the results from animal studies with Nav1.7 blockers translate into the clinic for treating a variety of pain etiologies.

Several high-affinity ligands for Nav1 channels have been identified and characterized. The guanidinium toxins tetrodotoxin and saxitoxin have been used extensively to characterize sodium channels and investigate their physiological roles. However, tetrodotoxin and saxitoxin bind to a region of the channel that is not involved in conferring state-dependent block, which is believed to be critical for achieving functional selectivity. Other radioligands have been identified, but they either are not selective for sodium channels over certain potassium or calcium channels, as is the case for [<sup>3</sup>H]WIN 17317-3 and [<sup>3</sup>H]lifaxazine (37, 49), or require coapplication of another ligand to enhance specific binding, which may complicate the resulting pharmacology (e.g., [<sup>3</sup>H]-batrachotoxin) (38). Recently, [<sup>3</sup>H]BPBTS binding to native rat brain and hNav1.5 channels was characterized and shown to display unique features, suggesting a distinct mechanism of interaction of BPBTS with the channel (29). However, binding of [<sup>3</sup>H]BPBTS to hNav1.7 channels could not be detected under identical experimental conditions. The results with [<sup>3</sup>H]BNZA illustrated in this study clearly indicate the utility of this ligand for studying Nav1.7 channels and defining their pharmacology. Since binding of [<sup>3</sup>H]BNZA

can also be demonstrated to other Nav1 channels, such as Nav1.5 and those present in brain tissue, [<sup>3</sup>H]BNZA could also be useful for identifying subtype-selective Nav1 channel modulators.

Local anesthetics, antiarrhythmics, and antiepileptic Nav1 blocking drugs bind to overlapping receptor sites that are located in the inner cavity of the pore of the sodium channel (8). Although residues in the IVS6 segment play a critical role in drug binding, other amino acid residues in IS6 and IIS6 also contribute to the receptor site for these drugs. A detailed knowledge of the site of interaction of 1-benzazepin-2-ones with Nav1 channels will require extensive mutagenesis studies, similar to those used above, to identify those residues that contribute to the high-affinity site of this new class of Nav1 inhibitors. Nonetheless, it is tempting to speculate that 1-benzazepin-2-ones may also share some of the same determinants that are associated with the interaction of local anesthetics, antiarrhythmics, and antiepileptic drugs with Nav1 channels. The fact that all these agents compete for [<sup>3</sup>H]BNZA binding to Nav1 channels is consistent with the existence of overlapping binding sites for these agents. However, the much higher affinity of 1-benzazepin-2-ones for Nav1 channels also suggests the existence of specific and well-defined interactions that could provide the basis for Nav1 subtype selectivity.

Clinically used sodium channel blockers preferentially bind to the open and inactivated states of sodium channels. 1-Benzazepin-2-one compounds share this mechanism of action and are at least 2 orders of magnitude more potent than currently available drugs as inhibitors of Nav1.7 channels. These data suggest that analogues that display selectivity over cardiac Nav1.5 channels and display appropriate pharmacokinetic and drug metabolism properties could be developed for the treatment of various pain conditions, including inflammatory and neuropathic pain states.

## ACKNOWLEDGMENT

We thank Drs. Catherine Abbadie, Euan MacIntyre, Owen McManus, William Martin, Robert Slaughter, McHardy Smith, and Ann Weber for advice and helpful discussions during the course of this study.

## REFERENCES

1. Catterall, W. A. (1992) Cellular and molecular biology of voltage-gated sodium channels, *Physiol. Rev.* 72, S15–48.
2. Isom, L. L. (2001) Sodium channel beta subunits: anything but auxiliary, *Neuroscientist* 7, 42–54.
3. Isom, L. L., Scheuer, T., Brownstein, A. B., Ragsdale, D. S., Murphy, B. J., and Catterall, W. A. (1995) Functional co-expression of the beta 1 and type IIA alpha subunits of sodium channels in a mammalian cell line, *J. Biol. Chem.* 270, 3306–3312.
4. Isom, L. L., De Jongh, K. S., Patton, D. E., Reber, B. F., Offord, J., Charbonneau, H., Walsh, K., Goldin, A. L., and Catterall, W. A. (1992) Primary structure and functional expression of the beta 1 subunit of the rat brain sodium channel, *Science* 256, 839–842.
5. Shah, B. S., Stevens, E. B., Gonzalez, M. I., Bramwell, S., Pinnock, R. D., Lee, K., and Dixon, A. K. (2000) beta3, a novel auxiliary subunit for the voltage-gated sodium channel, is expressed preferentially in sensory neurons and is upregulated in the chronic constriction injury model of neuropathic pain, *Eur. J. Neurosci.* 12, 3985–3990.

6. Vijayaragavan, K., O'Leary, M. E., and Chahine, M. (2001) Gating properties of Na(v)1.7 and Na(v)1.8 peripheral nerve sodium channels, *J. Neurosci.* 21, 7909–7918.
7. Goldin, A. L., Barchi, R. L., Calwell, J. H., Hofmann, F., Howe, J. R., Hunter, J. C., Kallen, R. G., Mandel, G., Meisler, M. H., Netter, Y. B., Noda, M., Tamkun, M. M., Waxman, S. G., Wood, J. N., and Catterall, W. A. (2000) Nomenclature of voltage-gated sodium channels, *Neuron* 28, 165–368.
8. Catterall, W. A., Goldin, A. L., Waxman, S. G., and International-Union-of-Pharmacology. (2003) International Union of Pharmacology. XXXIX. Compendium of voltage-gated ion channels: sodium channels, *Pharmacol. Rev.* 55, 575–578.
9. Clare, J. J., Tate, S. N., Nobbs, M., and Romanos, M. A. (2000) Voltage-gated sodium channels as therapeutic targets, *Drug Discovery Today* 5, 506–520.
10. Ragsdale, D. S., McPhee, J. C., Scheuer, T., and Catterall, W. A. (1996) Common molecular determinants of local anesthetic, antiarrhythmic, and anticonvulsant block of voltage-gated Na<sup>+</sup> channels, *Proc. Natl. Acad. Sci. U.S.A.* 93, 9270–9275.
11. Zimanyi, I., Weiss, S. R., Lajtha, A., Post, R. M., and Reith, M. E. (1989) Evidence for a common site of action of lidocaine and carbamazepine in voltage-dependent sodium channels, *Eur. J. Pharmacol.* 167, 419–422.
12. Kohling, R. (2002) Voltage-gated sodium channels in epilepsy, *Epilepsia* 43, 1278–1295.
13. Scholz, A. (2002) Mechanisms of (local) anaesthetics on voltage-gated sodium and other ion channels, *Br. J. Anaesth.* 89, 52–61.
14. di-Vadi, P. P., and Hamann, W. (1998) The use of lamotrigine in neuropathic pain, *Anaesthesia* 53, 808–809.
15. Rizzo, M. A. (1997) Successful treatment of painful traumatic mononeuropathy with carbamazepine: insights into a possible molecular pain mechanism, *J. Neurol. Sci.* 152, 103–106.
16. Ross, E. L. (2000) The evolving role of antiepileptic drugs in treating neuropathic pain, *Neurology* 55, S41–46, discussion S54–48.
17. Argoff, C. E. (2000) New analgesics for neuropathic pain: the lidocaine patch, *Clin. J. Pain* 16, S62–66.
18. Black, J. A., Liu, S., Tanaka, M., Cummins, T. R., and Waxman, S. G. (2004) Changes in the expression of tetrodotoxin-sensitive sodium channels within dorsal root ganglia neurons in inflammatory pain, *Pain* 108, 237–247.
19. Nassar, M. A., Stirling, L. C., Forlani, G., Baker, M. D., Matthews, E. A., Dickenson, A. H., and Wood, J. N. (2004) Nociceptor-specific gene deletion reveals a major role for Nav1.7 (PN1) in acute and inflammatory pain, *Proc. Natl. Acad. Sci. U.S.A.* 101, 12706–12711.
20. Waxman, S. G., and Dib-Hajj, S. (2005) Erythralgia: molecular basis for an inherited pain syndrome, *Trends Mol. Med.* 11, 555–562.
21. Waxman, S. G., and Dib-Hajj, S. D. (2005) Erythromelalgia: a hereditary pain syndrome enters the molecular era, *Ann. Neurol.* 57, 785–788.
22. Fertleman, C. R., Baker, M. D., Parker, K. A., Moffatt, S., Elmslie, F. V., Abrahamsen, B., Ostman, J., Klugbauer, N., Wood, J. N., Gardiner, R. M., and Rees, M. (2006) SCN9A mutations in paroxysmal extreme pain disorder: allelic variants underlie distinct channel defects and phenotypes, *Neuron* 52, 767–774.
23. Cox, J. J., Reimann, F., Nicholas, A. K., Thornton, G., Roberts, E., Springell, K., Karbani, G., Jafri, H., Mannan, J., Raashid, Y., Al-Gazali, L., Hamamy, H., Valente, E. M., Gorman, S., Williams, R., McHale, D. P., Wood, J. N., Gribble, F. M., and Woods, C. G. (2006) An SCN9A channelopathy causes congenital inability to experience pain, *Nature* 444, 894–898.
24. Goldberg, Y. P., MacFarlane, J., MacDonald, M. L., Thompson, J., Dube, M. P., Mattice, M., Fraser, R., Young, C., Hossain, S., Pape, T., Payne, B., Radomski, C., Donaldson, G., Ives, E., Cox, J., Youngusband, H. B., Green, R., Duff, A., Boltshauser, E., Grinspan, G. A., Dimon, J. H., Sibley, B. G., Andria, G., Toscano, E., Kerdraon, J., Bowsher, D., Pimstone, S. N., Samuels, M. E., Sherrington, R., and Hayden, M. R. (2007) Loss-of-function mutations in the Nav1.7 gene underlie congenital indifference to pain in multiple human populations, *Clin. Genet.* 71, 311–319.
25. Gonzalez, J. E., Oades, K., Leychikis, Y., Harootunian, A., and Negulescu, P. A. (1999) Cell-based assays and instrumentation for screening ion-channel targets, *Drug Discovery Today* 4, 431–439.
26. Schroeder, K., Neagle, B., Trezise, D. J., and Worley, J. (2003) Ionworks HT: a new high-throughput electrophysiology measurement platform, *J. Biomol. Screening* 8, 50–64.
27. Felix, J. P., Williams, B. S., Priest, B. T., Brochu, R. M., Dick, I. E., Warren, V. A., Yan, L., Slaughter, R. S., Kaczorowski, G. J., Smith, M. M., and Garcia, M. L. (2004) Functional assay of voltage-gated sodium channels using membrane potential-sensitive dyes, *Assay Drug Dev. Technol.* 2, 260–268.
28. Liu, C. J., Priest, B. T., Bugianesi, R. M., Dulski, P. M., Felix, J. P., Dick, I. E., Brochu, R. M., Knaus, H. G., Middleton, R. E., Kaczorowski, G. J., Slaughter, R. S., Garcia, M. L., and Kohler, M. G. (2006) A high-capacity membrane potential FRET-based assay for Nav1.8 channels, *Assay Drug Dev. Technol.* 4, 37–48.
29. Priest, B. T., Garcia, M. L., Middleton, R. E., Brochu, R. M., Clark, S., Dai, G., Dick, I. E., Felix, J. P., Liu, C. J., Reisetter, B. S., Schmalhofer, W. A., Shao, P. P., Tang, Y. S., Chou, M. Z., Kohler, M. G., Smith, M. M., Warren, V. A., Williams, B. S., Cohen, C. J., Martin, W. J., Meinke, P. T., Parsons, W. H., Wafford, K. A., and Kaczorowski, G. J. (2004) A disubstituted succinamide is a potent sodium channel blocker with efficacy in a rat pain model, *Biochemistry* 43, 9866–9876.
30. Brochu, R. M., Dick, I. E., Tarpley, J. W., McGowan, E., Gunner, D., Herrington, J., Shao, P. P., Ok, D., Li, C., Parsons, W. H., Stump, G. L., Regan, C. P., Lynch, J. J., Jr., Lyons, K. A., McManus, O. B., Clark, S., Ali, Z., Kaczorowski, G. J., Martin, W. J., and Priest, B. T. (2006) Block of peripheral nerve sodium channels selectively inhibits features of neuropathic pain in rats, *Mol. Pharmacol.* 69, 823–832.
31. Hoyt, S. B., London, C., Gorin, D., Wyvratt, M. J., Fisher, M. H., Abbadie, C., Felix, J. P., Garcia, M. L., Li, X., Lyons, K. A., McGowan, E., Macintyre, D. E., Martin, W. J., Priest, B. T., Ritter, A., Smith, M. M., Warren, V. A., Williams, B. S., Kaczorowski, G. J., and Parsons, W. H. (2007) Discovery of a novel class of benzazepinone Na(v)1.7 blockers: Potential treatments for neuropathic pain, *Bioorg. Med. Chem. Lett.* 17, 4630–4634.
32. Hoyt, S. B., London, C., Ok, H. O., Gonzalez, E., Duffy, J. L., Abbadie, C., Dean, B. J., Felix, J. P., Garcia, M. L., Jochowitz, N., Karanam, B. V., Li, X., Lyons, K. A., McGowan, E. M., Macintyre, D. E., Martin, W. J., Priest, B. T., Smith, M. M., Tschirret-Guth, R. A., Warren, V. A., Williams, B. S., Kaczorowski, G. J., and Parsons, W. H. (2007) Benzazepinone Nav1.7 blockers: potential treatments for neuropathic pain, *Bioorg. Med. Chem. Lett.* (in press).
33. Hamill, O. P., Marty, A., Neher, E., Sakmann, B., and Sigworth, F. J. (1981) Improved patch-clamp techniques for high-resolution current recording from cells and cell-free membrane patches, *Pfluegers Arch.* 391, 85–100.
34. Knaus, H. G., Koch, R. O., Eberhart, A., Kaczorowski, G. J., Garcia, M. L., and Slaughter, R. S. (1995) [125I]margatoxin, an extraordinarily high affinity ligand for voltage-gated potassium channels in mammalian brain, *Biochemistry* 34, 13627–13634.
35. Hille, B. (1977) Local anesthetics: hydrophilic and hydrophobic pathways for the drug-receptor reaction, *J. Gen. Physiol.* 69, 497–515.
36. Bean, B. P., Cohen, C. J., and Tsien, R. W. (1983) Lidocaine block of cardiac sodium channels, *J. Gen. Physiol.* 81, 613–642.
37. Wanner, S. G., Glossmann, H., Knaus, H. G., Baker, R., Parsons, W., Rupprecht, K. M., Brochu, R., Cohen, C. J., Schmalhofer, W., Smith, M., Warren, V., Garcia, M. L., and Kaczorowski, G. J. (1999) WIN 17317-3, a new high-affinity probe for voltage-gated sodium channels, *Biochemistry* 38, 11137–11146.
38. Catterall, W. A., Morrow, C. S., Daly, J. W., and Brown, G. B. (1981) Binding of batrachotoxin A 20- $\alpha$ -benzoate to a receptor site associated with sodium channels in synaptic nerve ending particles, *J. Biol. Chem.* 256, 8922–8927.
39. Finnerup, N. B., Biering-Sorensen, F., Johannesen, I. L., Terkelsen, A. J., Juhl, G. I., Kristensen, A. D., Sindrup, S. H., Bach, F. W., and Jensen, T. S. (2005) Intravenous lidocaine relieves spinal cord injury pain: a randomized controlled trial, *Anesthesiology* 102, 1023–1030.
40. Harty, T. P., Dib-Hajj, S. D., Tyrrell, L., Blackman, R., Hisama, F. M., Rose, J. B., and Waxman, S. G. (2006) Na(V)1.7 mutant A863P in erythromelalgia: effects of altered activation and steady-state inactivation on excitability of nociceptive dorsal root ganglion neurons, *J. Neurosci.* 26, 12566–12575.
41. Yang, Y., Wang, Y., Li, S., Xu, Z., Li, H., Ma, L., Fan, J., Bu, D., Liu, B., Fan, Z., Wu, G., Jin, J., Ding, B., Zhu, X., and Shen, Y. (2004) Mutations in SCN9A, encoding a sodium channel  $\alpha$  subunit, in patients with primary erythromelalgia, *J. Med. Genet.* 41, 171–174.
42. Drenth, J. P., te Morsche, R. H., Guillet, G., Taieb, A., Kirby, R. L., and Jansen, J. B. (2005) SCN9A mutations define primary

- erythromelgia as a neuropathic disorder of voltage gated sodium channels, *J. Invest. Dermatol.* 124, 1333–1338.
43. Michiels, J. J., te Morsche, R. H., Jansen, J. B., and Drenth, J. P. (2005) Autosomal dominant erythromelgia associated with a novel mutation in the voltage-gated sodium channel alpha subunit Nav1.7, *Arch. Neurol.* 62, 1587–1590.
44. Dib-Hajj, S. D., Rush, A. M., Cummins, T. R., Hisama, F. M., Novella, S., Tyrrell, L., Marshall, L., and Waxman, S. G. (2005) Gain-of-function mutation in Nav1.7 in familial erythromelgia induces bursting of sensory neurons, *Brain* 128, 1847–1854.
45. Han, C., Rush, A. M., Dib-Hajj, S. D., Li, S., Xu, Z., Wang, Y., Tyrrell, L., Wang, X., Yang, Y., and Waxman, S. G. (2006) Sporadic onset of erythromelgia: a gain-of-function mutation in Nav1.7, *Ann. Neurol.* 59, 553–558.
46. Davis, M. D., and Sandroni, P. (2005) Lidocaine patch for pain of erythromelgia: follow-up of 34 patients, *Arch. Dermatol.* 141, 1320–1321.
47. Kuhnert, S. M., Phillips, W. J., and Davis, M. D. (1999) Lidocaine and mexiletine therapy for erythromelgia, *Arch. Dermatol.* 135, 1447–1449.
48. Fertleman, C. R., and Ferrie, C. D. (2006) What's in a name—familial rectal pain syndrome becomes paroxysmal extreme pain disorder, *J. Neurol., Neurosurg. Psychiatry* 77, 1294–1295.
49. MacKinnon, A. C., Wyatt, K. M., McGivern, J. G., Sheridan, R. D., and Brown, C. M. (1995) [3H]-lifarizine, a high affinity probe for inactivated sodium channels, *Br. J. Pharmacol.* 115, 1103–1109.

B17018207